Contribution from Ames Laboratory and the Department of Chemistry,
Iowa State University, Ames, Iowa 50011

# Structure and Reactivity of Novel Alkylcobalt Macrocycles

Shaoyung Lee, James H. Espenson,* and Andreja Bakac*

*Received October 5, 1989*

The organocobalt complexes $[(H_2O)LCoR](ClO_4)_2$ [R = primary alkyl, substituted primary alkyl; L = $Me_6[14]4,11\text{-diene}N_4$ ($L^1$), *C-meso*-$Me_6[14]aneN_4$ ($L^2$)] were prepared photochemically from the corresponding alkylcobaloximes. A modified Fenton reaction also yielded the organocobalt complexes. The complexes were characterized by $^1H$ NMR and visible spectroscopies and crystal structure determination for [*N-rac*-$(H_2O)L^1CoCH_2Cl](ClO_4)_2$. The complex crystallizes in the monoclinic space group $P2_1/c$ with $Z = 4$. The unit cell dimensions are $a = 15.315$ (2) Å, $b = 9.012$ (3) Å, $c = 18.998$ (5) Å, $\beta = 105.47$ (2)°, and $V = 2527$ (2) Å$^3$ ($R = 0.0394$, $R_w = 0.0497$). The alkylcobalt complexes (R = $C_2H_5$, *n*-$C_3H_7$) undergo unimolecular homolysis; the activation enthalpy for this process is 24–26 kcal/mol. The rates of the alkyl group transfer between $Cr^{2+}$ and $LCoR^{2+}$ in $H_2O$ show a strong dependence on steric effects of the alkyl group, consistent with an $S_H2$ mechanism.

## Introduction

Since the discovery that coenzyme $B_{12}$ contains a cobalt–carbon bond,[1] a large number of model compounds containing a Co–C bond have been prepared and characterized.[2-4] We recently developed a photochemical method for the preparation of a series of $(H_2O)([14]aneN_4)CoR^{2+}$ complexes[5] (Scheme I). The efficiency of capture of the radical is quite high, giving a nearly quantitative yield (≥90%) of $(H_2O)([14]aneN_4)CoR^{2+}$ complexes in solution, as judged spectrophotometrically. The success of the method derives in part from the high molar absorptivities of the organocobaloximes because the product, itself photochemically sensitive to Co–C cleavage, is thus protected from light.

### Scheme I

$$py(dmgH)_2CoR \xrightarrow[H_2O]{h\nu} (H_2O)pyCo(dmgH)_2 + R^\bullet \quad \text{(I-1)}$$

$$(H_2O)pyCo(dmgH)_2 \xrightarrow{H^+} Co_{aq}^{2+} + 2dmgH_2 + pyH^+ \quad \text{(I-2)}$$

$$R^\bullet + (H_2O)_2LCo^{2+} \rightarrow (H_2O)LCoR^{2+} + H_2O \quad \text{(I-3)}$$

R = primary or substituted primary alkyl

We have now prepared several new organocobalt complexes with macrocyclic ligands $Me_6[14]4,11\text{-diene}N_4$ ($L^1$) and *C-meso*-$Me_6[14]aneN_4$ ($L^2$), as shown in Figure 1. Both *N-meso*- and *N-rac*-organocobalt complexes of the former ligand have been observed in this work.

The six methyl groups on the macrocycles add steric hindrance at the metal center. This is probably the reason why the $E°$ value for the $L^2Co^{3+/2+}$ couple is ~0.2 V higher than that of $[14]aneN_4Co(H_2O)_2^{3+/2+}$;[6] indeed, this effect more than offsets the electronic effect on $E°$ expected from the incorporation of six methyl groups.

The new complexes were examined for their reactivity in unimolecular[7-14] and bimolecular[15-20] homolysis. Both pathways, especially the former, are important in determining metal–carbon bond dissociation enthalpies (BDE). The approach is based on the assumption that the BDE can be approximated as $\Delta H^\ddagger$ for the unimolecular homolysis since the recombination reaction is assumed to have a negligibly small activation enthalpy,[9a] although that is not universally true.[9b] We anticipated a reasonably rapid homolysis of the new complexes based on the reported photochemical threshold energies for a number of methylcobalt complexes,[21] including $(H_2O)L^1CoCH_3^{2+}$.

All the cobalt(II) complexes in this work are presumably hexacoordinated in solution, with molecules of $H_2O$ completing the coordination sphere. In what follows the coordinated waters will be omitted.

## Experimental Section

**Reagents.** Organocobaloximes were prepared by a literature method.[22] The macrocycle 5,7,7,12,14,14-hexamethyl-1,4,8,11-tetraazacyclotetradeca-4,11-diene ($L^1$) was prepared by condensation of 1,2-diaminoethane and acetone as previously reported.[23] *C-meso*-5,7,7,12,14,14-Hexamethyl-1,4,8,11-tetrazacyclotetradecane ($L^2$) was prepared by borohydride reduction of the diene.[23] The cobalt macrocycles were prepared from anhydrous cobalt chloride and the desired macrocycle by a published procedure.[24]

Chromium(II) perchlorate solutions were prepared by reduction of aqueous $Cr(ClO_4)_3$ over zinc amalgam. The 4-hydroxy-2,2,6,6-tetramethylpiperidinyl-1-oxy free radical was used as purchased (Aldrich). The sample of $ABTS^{2-}$ (2,2′-azinobis(3-ethylbenzthiazoline-6-sulfonic acid) ammonium salt) was converted to the $ABTS^{\bullet-}$ radical by oxidation with cerium(IV) perchlorate.[25] The concentration of the $ABTS^{\bullet-}$ radical

---

(1) Lenhart, P. G.; Hodgkin, D. C. *Nature (London)* **1961**, *192*, 937.

(2) For recent reviews, see: (a) Toscano, P. J.; Marzilli, L. G. *Prog. Inorg. Chem.* **1984**, *31*, 105. (b) Pratt, J. M. *Chem. Soc. Rev.* **1985**, 161. (c) Halpern, J. *Science* **1985**, *227*, 869. (d) Finke, R. D.; Schiraldi, D. A.; Mayer, B. A. *Coord. Chem. Rev.* **1984**, *54*, 1. (e) Golding, B. T. J. R. *Neth. Chem. Soc.* **1987**, *106*, 342. (f) Bresciani Pahor, N.; Forcolin, M.; Marzilli, L. G.; Randaccio, L.; Summers, M. F.; Toscano, P. J. *Coord. Chem. Rev.* **1985**, *63*, 1. (g) Randaccio, L.; Bresciani Pahor, N.; Zangrando, E.; Marzilli, L. G. *Chem. Soc. Rev.* **1989**, *18*, 225.

(3) Roche, T. S.; Endicott, J. F. *J. Am. Chem. Soc.* **1972**, *94*, 8622.

(4) Roche, T. S.; Endicott, J. F. *Inorg. Chem.* **1974**, *13*, 1575.

(5) Bakac, A.; Espenson, J. H. *Inorg. Chem.* **1987**, *26*, 4353.

(6) Heckman, R. A.; Espenson, J. H. *Inorg. Chem.* **1979**, *18*, 38.

(7) Nohr, R. S.; Espenson, J. H. *J. Am. Chem. Soc.* **1975**, *97*, 3392.

(8) (a) Kirker, G. W.; Bakac, A.; Espenson, J. H. *J. Am. Chem. Soc.* **1982**, *104*, 1249. (b) Espenson, J. H.; Connolly, P.; Meyerstein, D.; Cohen, H. *Inorg. Chem.* **1983**, *22*, 1009. (c) Bakac, A.; Espenson, J. H. *J. Am. Chem. Soc.* **1984**, *106*, 5197.

(9) (a) Ng, F. T. T.; Rempel, G. L.; Halpern, J. *J. Am. Chem. Soc.* **1982**, *104*, 621. (b) Halpern, J.; Ng, F. T. T.; Rempel, G. L. *J. Am. Chem. Soc.* **1979**, *101*, 7124. (c) Halpern, J. *Acc. Chem. Res.* **1982**, *15*, 238. (d) Meyerstein, D.; Schwarz, H. A. *J. Chem. Soc., Faraday Trans. 1* **1988**, *84*, 2933.

(10) Grate, G. W.; Schrauzer, G. N. *Organometallics* **1982**, *1*, 1155.

(11) Tamblyn, W. H.; Klingler, R. J.; Hwang, W. S.; Kochi, J. K. *J. Am. Chem. Soc.* **1981**, *103*, 3161.

(12) Pohl, M. C.; Espenson, J. H. *Inorg. Chem.* **1980**, *19*, 235.

(13) Mulac, W. A.; Cohen, H.; Meyerstein, D. *Inorg. Chem.* **1982**, *21*, 4016.

(14) Fergusson, S. B.; Baird, M. C. *Inorg. Chim. Acta* **1982**, *63*, 41.

(15) Van den Bergen, A.; West, B. O. *J. Organomet. Chem.* **1974**, *64*, 1125.

(16) (a) Espenson, J. H.; Shveima, J. S. *J. Am. Chem. Soc.* **1973**, *95*, 4468. (b) Espenson, J. H.; Sellers, T. D., Jr. *J. Am. Chem. Soc.* **1974**, *96*, 94. (c) Espenson, J. H.; Leslie, J. P., II. *J. Am. Chem. Soc.* **1974**, *96*, 1954.

(17) Dizikes, L. J.; Ridley, W. P.; Wood, J. M. *J. Am. Chem. Soc.* **1978**, *100*, 1010.

(18) Parris, M.; Ashbrook, A. W. *Can. J. Chem.* **1979**, *57*, 1233.

(19) Chrzastowski, J. Z.; Cooksey, C. J.; Johnson, M. D.; Lockman, B. L.; Steggles, P. N. *J. Am. Chem. Soc.* **1975**, *97*, 932.

(20) Dodd, D.; Johnson, M. D.; Lockman, B. L. *J. Am. Chem. Soc.* **1977**, *99*, 3664.

(21) Endicott, J. F.; Balakrishnan, K. P.; Wong, C.-L. *J. Am. Chem. Soc.* **1980**, *102*, 5519.

(22) Schrauzer, G. N. *Inorg. Synth.* **1965**, *11*, 65.

(23) Hay, R. W.; Lawrance, G. A.; Curtis, N. F. *J. Chem. Soc., Perkin Trans. 1* **1975**, 591.

(24) Rillema, D. P.; Endicott, J. F.; Papaconstantinou, E. *Inorg. Chem.* **1971**, *10*, 1739.

(25) Maruthamuthu, P.; Venkatasubramanian, L.; Dharmalingam, P. *Bull. Chem. Soc. Jpn.* **1987**, *60*, 1113.

0020-1669/90/1329-3442$02.50/0

**Table I.** Spectral Data for $LCoR^{2+}$ Complexes

| complex | $\lambda_1$ ($\epsilon_1$)[a] | $\lambda_2$ ($\epsilon_2$)[a] | $\delta$(R), ppm[b] | $\delta$($CH_3$ (L)), ppm[b] |
|---|---|---|---|---|
| $(H_2O)L^1CoCH_3^{2+}$ | 470 (214)<br>470 (228)[c] | 376 (391)<br>376 (404)[c] | 1.61 (3 H) | 2.18 (6 H), 1.25 (6 H), 1.12 (3 H), 0.99 (3 H) |
| $(H_2O)L^1CoC_2H_5^{2+}$ | 480 (185) | 380 (401) | 0.10 (3 H, t) | 2.19 (6 H), 1.28 (6 H), 1.12 (3 H), 1.08 (3 H) |
| $(H_2O)L^1CoC_3H_7^{2+}$ | 480 (156) | 381 (345) | | 2.10 (6 H), 1.26 (6 H), 1.13 (3 H), 1.08 (3 H) |
| $(H_2O)L^1CoCH_2Cl^{2+}$ | 466 (152) | 356 (280) | | 2.19 (6 H), 1.30 (6 H), 1.03 (6 H) |
| $(H_2O)L^1CoCH_2OH^{2+}$ | 464 (168) | 373 (358) | | 2.04 (6 H), 1.21 (6 H), 1.03 (3 H), 0.82 (3 H) |
| $(H_2O)L^1CoCH_2OCH_3^{2+}$ | 466 (172) | 364 (366) | 3.15 (3 H, s) | 2.15 (6 H), 1.21 (6 H), 1.10 (3 H), 0.88 (3 H) |
| $(H_2O)L^2CoCH_3^{2+}$ | 498 (74)[c] | 384 (133)[c] | 2.01 (3 H, s) | 1.04–1.13 (15 H), 0.95 (3 H) |
| $(H_2O)L^2CoC_2H_5^{2+}$ | 504 (57) | 392 (115) | 0.28 (3 H, t) | 1.03–1.11 (15 H), 0.91 (3 H) |
| $(H_2O)L^2CoC_3H_7^{2+}$ | 508 (58) | 390 (134) | | 1.0–1.12 (15 H), 0.92 (3 H) |
| $(H_2O)L^2CoCH_2Cl^{2+}$ | 488 (79) | 372 (144) | | 1.03–1.16 (15 H), 0.87 (3 H) |

[a] In 0.01 M $HClO_4$; $\lambda$ in nm, $\epsilon$ in $M^{-1}$ $cm^{-1}$. [b] In $D_2O$ with HOD as the reference at $\delta$ 4.63 ppm. [c] Reference 4.

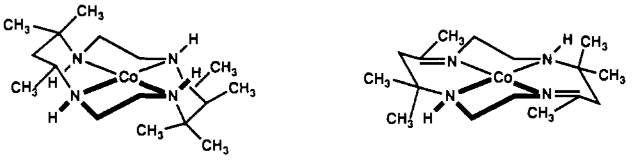

$Co(C\text{-}meso\text{-}Me_6[14]aneN_4)^{2+}$ $N\text{-}meso\text{-}Co(Me_6[14]4,11\text{-}dieneN_4)^{2+}$

**Figure 1.** Structures of the cobalt macrocycles.

was determined spectrophotometrically at 650 nm ($\epsilon$ 10050 L $mol^{-1}$ $cm^{-1}$).[25] Various hydroperoxides (2-methyl-2-butyl, 2,3-dimethyl-2-butyl, and 2-methyl-1-phenylpropyl) were prepared from the corresponding alcohols as previously described[26] and characterized by $^1H$ NMR spectroscopy. The concentrations of the hydroperoxides were determined spectrophotometrically by measuring the extent of formation of the derived organochromium(III) cations. Other materials were reagent grade and were used as purchased.

**Syntheses of Organocobalt Complexes $[LCoR](ClO_4)_2$.** Two routes were developed for this synthesis. One method involves the photolysis of acidic aqueous solutions of the appropriate organocobaloxime in the presence of $LCo^{2+}$.[5] The stirred suspension of organocobaloxime and $LCo^{2+}$ was cooled and irradiated by use of a 300-W sun lamp until all the organocobaloxime was consumed. The solid $dmgH_2$ produced was removed by filtration and some $NaClO_4$ added to filtrate. This caused immediate precipitation of $LCoR(ClO_4)_2$. The material was filtered out, washed with ether, and air-dried. In some cases the product was recrystallized from acidic ($HClO_4$) solution. All the complexes were characterized by their $^1H$ NMR spectra.

A second synthetic route was used for a few complexes; the hydroxymethyl–, methoxymethyl–, and methyl–$L^1$–cobalt complexes were prepared by a Fenton reaction from $L^1Co^{2+}$ and hydrogen peroxide in the presence of methanol, dimethyl ether, or dimethyl sulfoxide, respectively. The methyl complexes were also obtained from the reaction between *tert*-butyl hydroperoxide and $LCo^{2+}$.[27]

**Spectroscopy and Kinetics.** UV–visible spectra and single-wavelength absorbance vs time data were acquired by using a Cary Model 219 spectrophotometer or a Cary Model 14 spectrophotometer interfaced with an OLIS 3820 data system. Temperature control of ±0.1 °C was maintained by circulating water from a constant-temperature bath through the jacket of a water-filled cell holder. Fitting of kinetic data was done with a nonlinear least-squares program or standard first-order routines of the OLIS computer system.

Routine $^1H$ NMR spectra were collected with a Nicolet NT-300 spectrometer. The NMR experiments were all done in $D_2O$ with HOD as the reference at 4.63 ppm. Gas chromatography was carried out by use of a Hewlett-Packard 5790A series gas chromatograph with a 3390 integrator. A VZ-10 column was used for the determinations.

**X-ray Crystallography.** A single crystal of $[(H_2O)L^1CoCH_2Cl](ClO_4)_2$ for X-ray crystal structure determination was grown in an open vial at room temperature from a neutral aqueous solution that originally contained 5 mM $[N\text{-}meso\text{-}L^1CoCH_2Cl](ClO_4)_2$. Under these conditions the N-meso complex isomerizes rapidly (<5 min) to the N-racemic form; see later. An orange-yellow crystal of the resulting $[N\text{-}rac\text{-}(H_2O)L^1CoCH_2Cl](ClO_4)_2$ was mounted on a glass fiber in a random orientation and moved into the cold stream of the low-temperature device on the diffractometer. The cell constants were determined from a list of reflections found by an automated search routine.

**Table II.** Crystallographic Data for $[N\text{-}rac\text{-}(H_2O)L^1CoCH_2Cl](ClO_4)_2$

| | | | |
|---|---|---|---|
| empirical formula | $CoC_{17}H_{36}Cl_3N_4O_9$ | fw | 605.79 |
| *a*, Å | 15.315 (2) | space group | $P2_1/c$ (No. 14) |
| *b*, Å | 9.012 (3) | *T* | −30 °C |
| *c*, Å | 18.998 (5) | $\lambda$ | 0.71073 Å |
| $\beta$, deg | 105.47 (2) | $\rho_{calcd}$ | 1.592 g $cm^{-3}$ |
| *V*, $Å^3$ | 2527 (2) | $\mu$ (Mo K$\alpha$) | 10.48 $cm^{-1}$ |
| *Z* | 4 | $R$, $R_w$ | 0.0394, 0.0497 |

A total of 3435 reflections were collected in the $+h,+k,\pm l$ quadrant, of which 3291 were unique and not systematically absent; of these, 2229 having $F_o^2 > 3\sigma(F_o^2)$ were used in the refinement. The agreement factor for the averaging of 186 observed reflections was 2.8% based on intensity. The intensities of three standards, checked hourly over the course of the data collection, indicated only random variations within the errors of the measurement. Lorentz and polarization corrections were applied. The space group $P2_1/c$ was uniquely defined by the observed systematic absences. The positions of all 34 non-hydrogen atoms were taken from a direct methods *E* map. Following isotropic least-squares refinement of all atoms, hydrogen atoms were added in calculated positions for all carbon atoms and used for the calculation of structure factors only. Since no initial absorption corrections were made, a numerical correction was made at this time on the unaveraged data set, and the data were reaveraged. In the final stage of refinement, the cobalt, chlorine, oxygen, and nitrogen atoms were given anisotropic temperature factors. Following convergence, the discrepancy indices were $R = 0.0421$ and $R_w = 0.0538$. A difference Fourier map was calculated, and the positions of the four highest peaks were found to correspond to the expected positions of hydrogen atoms on the water molecule coordinated to Co and on atoms N(1) and N(3). The positions of the four hydrogen atoms were then included in the refinement (isotropic thermal parameters were fixed for the hydrogen atoms).

The final cycle of refinement included 234 variable parameters and converged with unweighted and weighted agreement factors of $R = \sum|F_o - F_c|/\sum F_o = 0.0394$ and $R_w = [\sum w(F_o - F_c)^2/\sum w(F_o)^2]^{1/2} = 0.0497$. The standard deviation of an observation of unit weight was 1.29. The largest positive peak in the final difference Fourier had a height of 0.368 e/$Å^3$. Extinction corrections were not made.

X-ray data collection and structure solution were carried out at the Iowa State Molecular Structure Laboratory. All calculations were performed on a Digital Equipment Corp. MicroVAX II computer using the CAD4/SDP package.

## Results

**NMR and Optical Spectra.** The visible spectra of the alkyl complexes exhibit two weakly allowed transitions at 460–510 and 360–390 nm, as given in Table I. The spectra of the methyl complexes agree well with those reported previously.[4] The $^1H$ NMR spectra of the alkylcobalt complexes (Table I) also support the assigned structures.

**X-ray Structure of $[N\text{-}rac\text{-}(H_2O)L^1CoCH_2Cl](ClO_4)_2$.** The molecular structure of the cation consists of a six-coordinate cobalt ion, in which the cobalt is surrounded by four nitrogen atoms from the equatorial macrocyclic ligand with a water molecule and a chloromethyl group in the axial positions. The perchlorate anions are uncoordinated.

The structure of the complex is represented by the ORTEP diagram in Figure 2. The crystallographic data are collected in Table II. The calculated bond distances and bond angles are reported in Tables III and IV, respectively. The atomic coordinates

---

(26) (a) Milas, N. A.; Sugenor, D. M. *J. Am. Chem. Soc.* **1946**, *68*, 205. (b) Leslie, J. P., II; Espenson, J. H. *J. Am. Chem. Soc.* **1976**, *98*, 4839.

(27) Espenson, J. H.; Martin, A. H. *J. Am. Chem. Soc.* **1977**, *99*, 5953.

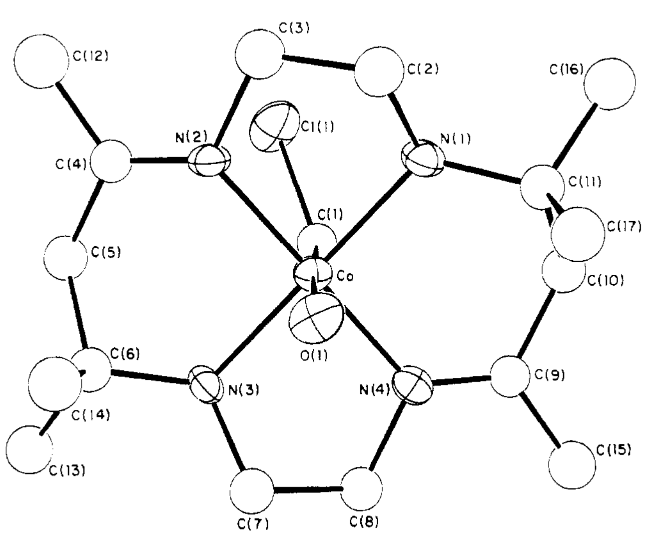

**Figure 2.** ORTEP diagram of *N-rac*-$(H_2O)L^1CoCH_2Cl^{2+}$.

**Table III.** Major Bond Distances (Å) for $[N\text{-}rac\text{-}(H_2O)L^1CoCH_2Cl](ClO_4)_2$

| | | | |
|---|---|---|---|
| Co-O1 | 2.062 (4) | N1-C2 | 1.499 (6) |
| Co-N1 | 1.985 (4) | N1-C11 | 1.510 (6) |
| Co-N2 | 1.923 (4) | N2-C3 | 1.480 (6) |
| Co-N3 | 1.981 (4) | N2-C4 | 1.275 (6) |
| Co-N4 | 1.919 (4) | N3-C6 | 1.504 (6) |
| Co-C1 | 1.965 (5) | N3-C7 | 1.481 (6) |
| Cl1-C1 | 1.796 (5) | N4-C8 | 1.481 (6) |
| O1-H1(O1) | 0.76 (7) | N4-C9 | 1.287 (6) |
| O1-H2(O1) | 0.62 (8) | | |

**Table IV.** Bond Angles (deg) in $[N\text{-}rac\text{-}(H_2O)L^1CoCH_2Cl](ClO_4)_2$

| | | | |
|---|---|---|---|
| O1-Co-N1 | 90.0 (2) | N1-C11-C10 | 107.6 (4) |
| O1-Co-N2 | 88.7 (1) | N1-C11-C16 | 108.3 (4) |
| O1-Co-N3 | 90.4 (2) | N1-C11-C17 | 113.1 (3) |
| O1-Co-N4 | 88.7 (1) | C10-C11-C16 | 108.3 (3) |
| O1-Co-C1 | 176.6 (2) | C10-C11-C17 | 110.0 (4) |
| N1-Co-N2 | 85.6 (1) | Co-N2-N4 | 128.1 (3) |
| N1-Co-N3 | 179.7 (2) | C3-N2-C4 | 119.0 (4) |
| N1-Co-N4 | 94.6 (1) | Co-N3-C6 | 120.8 (3) |
| N1-Co-C1 | 89.6 (1) | Co-N3-C7 | 105.7 (3) |
| N2-Co-N3 | 94.3 (2) | Co-N3-H(N3) | 105 (5) |
| N2-Co-N4 | 177.4 (1) | C6-N3-C7 | 115.8 (4) |
| N2-Co-C1 | 94.6 (2) | C6-N3-H(N3) | 101 (5) |
| N3-Co-N4 | 85.5 (2) | C7-N3-H(N3) | 108 (5) |
| N3-Co-C1 | 90.1 (2) | Co-N4-C8 | 111.9 (3) |
| N4-Co-C1 | 88.0 (1) | Co-N4-C9 | 128.7 (3) |
| Co-O1-H1(O1) | 129 (6) | C8-N4-C9 | 119.2 (4) |
| Co-O1-H2(O1) | 124 (8) | Co-C1-Cl1 | 115.4 (2) |
| H1(O1)-O1-H2(O1) | 107 (9) | N1-C2-C3 | 108.0 (4) |
| Co-N1-C2 | 106.0 (3) | N2-C3-C2 | 110.7 (4) |
| Co-N1-C11 | 121.1 (3) | N2-C4-C5 | 121.0 (5) |
| Co-N1-H(N1) | 102 (4) | N2-C4-C12 | 122.2 (5) |
| C2-N1-C11 | 114.2 (4) | C5-C4-C12 | 116.6 (4) |
| C2-N1-H(N1) | 106 (4) | C4-C5-C6 | 116.4 (4) |
| C11-N1-H(N1) | 106 (4) | N3-C6-C5 | 106.1 (3) |
| Co-N2-C3 | 112.4 (2) | N3-C6-C13 | 109.3 (4) |
| N4-C8-C7 | 109.3 (4) | N3-C6-C14 | 113.0 (4) |
| N4-C9-C10 | 121.2 (4) | C5-C6-C13 | 108.3 (4) |
| N4-C9-C15 | 123.1 (4) | C5-C6-C14 | 111.1 (4) |
| C10-C9-C15 | 115.7 (4) | C13-C6-C14 | 108.9 (3) |
| C9-C10-C11 | 117.9 (4) | N3-C7-C8 | 107.1 (4) |
| | | C16-C11-C17 | 109.3 (4) |

**Table V.** Kinetics and Organic Products of the Decomposition of *N-meso*-$L^1CoC_2H_5^{2+}$ in the Presence of Scavengers[a]

| scavenger | $10^4k_H$, $s^{-1}$ | product |
|---|---|---|
| $Cr^{2+}$ | 3.4[b] | $C_2H_6$ (~95%), $C_2H_4$ (~5%) |
| $Co(NH_3)_5Br^{2+}$ | 4.2[c] | $C_2H_5Br$, $C_2H_4$, $C_2H_6$ |
| $O_2$ | 3.9[d] | $C_2H_4$ (trace) |
| HTMPO | 4.7[d] | $C_2H_4$ |

[a] $T = 25.0 \pm 0.1$ °C. [b] $\mu = 0.14$ M. Extrapolated to $[Cr^{2+}] = 0$. [c] $\mu = 0.5$ M. [d] $\mu = 0.1$ M.

**Table VI.** Activation Parameters for Unimolecular Homolysis of Alkycobalt Complexes $LCoR^{2+}$

| $LCoR^{2+}$ | $\Delta H^*$, kcal $mol^{-1}$ | $\Delta S^*$, cal $mol^{-1}$ $K^{-1}$ |
|---|---|---|
| *N-meso*-$L^1CoC_2H_5^{2+}$ | $25.1 \pm 0.9$ | $10 \pm 3$ |
| *N-meso*-$L^1CoC_3H_7^{2+}$ | $26.6 \pm 0.9$ | $14 \pm 3$ |
| $L^2CoC_2H_5^{2+}$ | $25.6 \pm 0.6$ | $12 \pm 2$ |
| $L^2CoC_3H_7^{2+}$ | $26.5 \pm 0.8$ | $15 \pm 3$ |

and additional crystallograhpic data, as well as the stereoview of the cation, are given in the supplementary material.

**Isomerization of $L^1CoCH_3^{2+}$.** The Co–$CH_3$ singlet in the $^1H$ NMR spectrum is located at 1.65 and 1.38 ppm for the respective N-meso and N-racemic isomers in $D_2O$. The chemical shifts for this resonance in these two isomers are consistent with those found by Endicott and co-workers.[3] The initial spectrum is that of the nearly pure N-meso isomer. After sufficient time, 13 h, all of the N-meso isomer converts to the N-racemic isomer. Although an attempt to measure the isomerization rate has not been made, the relative rates are in the order $n$-$C_3H_7 > C_2H_5 > CH_3$, which shows that the rate is dependent on the bulk of the alkyl group bound to cobalt. This is due to the steric interaction between the axial methyl group in the ring and the alkyl group bound to cobalt. The isomerization of *N-meso*-$L^1CoCH_2Cl^{2+}$ to the N-racemic form at pH 7 is complete in the time necessary to dissolve the compound and run the NMR spectrum (<5 min).

**Homolysis of *N-meso*-$L^1CoR^{2+}$ and $L^2CoR^{2+}$.** Dilute aqueous solutions of the *N-meso*-$L^1CoC_2H_5^{2+}$ decompose at room temperature to yield equivalent amounts of $C_2H_4$ and $C_2H_6$. Very little (~3%) $n$-butane was formed, as compared to ~70% expected if the products arose from the self-reaction of ethyl radicals.[28] We interpret this to mean that the ethyl radical attacks the organometallic complex, especially since the concentration of ethyl radicals at steady state was low under these conditions. The product, by its visible spectrum, is the cobalt(II) macrocycle. The reactions suggested are shown in Scheme II. Similar observations were also made with the other organocobalt complexes with the exception of the methyl, which did not appear to homolyze under comparable conditions.

**Scheme II**

$$L^1CoC_2H_5^{2+} \rightarrow L^1Co^{2+} + C_2H_5^{\bullet} \quad k_H \qquad \text{(II-1)}$$

$$C_2H_5^{\bullet} + L^1CoC_2H_5^{2+} \rightarrow C_2H_4 + C_2H_6 + L^1Co^{2+} \qquad \text{(II-2)}$$

The rate of loss of *N-meso*-$L^1CoC_2H_5^{2+}$ is accelerated by $Cr^{2+}$, $Co(NH_3)_5Br^{2+}$, $O_2$, and HTMPO, i.e. by reagents that react rapidly with the ethyl radical. The kinetics of these reactions were studied under conditions where the scavenger is present in large excess. The reactions follow first-order kinetics in which $k_H$ is identified as the rate constant for homolysis of the cobalt–carbon bond, as in eq II-1. In accord with that, the rate constant shows no dependence on the concentration or identity of the scavenger, except for $Cr^{2+}$, where a second term with a first-order dependence on $[Cr^{2+}]$ is seen; extrapolation to $[Cr^{2+}] = 0$ affords another value of $k_H$. The products and rate constants are summarized in Table V.

The kinetics of homolysis were studied at different temperatures for the organocobalt complexes *N-meso*-$L^1CoR^{2+}$ and $L^2CoR^{2+}$ for R = $C_2H_5$ and $n$-$C_3H_7$. The data were fit to the Eyring equation in plots of ln $(k_H/T)$ against $1/T$. The values of $\Delta H^*$ and $\Delta S^*$ are listed in Table VI.

**Reaction of $CH_3^{\bullet}$ with *N-meso*-$L^1CoCH_3^{2+}$.** Evidence for this reaction came from the distribution of products in the reaction of $Fe_{aq}^{2+}$ with *tert*-amyl hydroperoxide in the presence of the methylcobalt complex. The kinetics of this reaction were then studied by laser flash photolysis.[29] $ABTS^{\bullet-}$ was used as the

---

(28) Bakac, A.; Espenson, J. H. *J. Phys. Chem.* **1986**, *90*, 325.

(29) (a) Hoselton, M. A.; Lin, C.-T.; Schwartz, H. A.; Sutin, N. *J. Am. Chem. Soc.* **1978**, *100*, 2383. (b) Connolly, P. Ph.D. Disertation, Iowa State University, Ames, Iowa, 1985.

competing chromophore. The reaction steps are the following:

$$L^1CoCH_3^{2+} \xrightarrow{h\nu} CH_3^{\bullet} + L^1Co^{2+} \quad (1)$$

$$CH_3^{\bullet} + L^1CoCH_3^{2+} \rightarrow C_2H_6 + L^1Co^{2+} \quad k_2 \quad (2)$$

$$CH_3^{\bullet} + CH_3^{\bullet} \rightarrow C_2H_6 \quad k_c \quad (3)$$

$$CH_3^{\bullet} + ABTS^{\bullet -} \rightarrow \text{products} \quad k_A \quad (4)$$

The methyl radical, formed by photohomolysis of the methylcobalt, reacts in three competing pathways, including the reaction of interest. The other rate constants can be determined in blank experiments with the methylcobalt complex at a low concentration where eq 2 is unimportant. The pseudo-first-order rate constant is given by eq 5 in a reaction that can be monitored by following

$$k_{obs} = k_2[N\text{-}meso\text{-}L^1CoCH_3^{2+}] + k_A[ABTS^{\bullet -}] + 2k_c[CH_3^{\bullet}]_{av} \quad (5)$$

the disappearance of $ABTS^{\bullet -}$ at 650 nm. A plot of $k_{cor}$ ($=k_{obs} - k_A[ABTS^{\bullet -}] - 2k_c[CH_3^{\bullet}]_{av}$) versus [*N-meso*-$L^1CoCH_3^{2+}$] is linear and gives the value $k_2 = (4.1 \pm 0.2) \times 10^7$ L mol$^{-1}$ s$^{-1}$.

**Reactions with $Cr^{2+}$.** The reactions involved are shown in eqs 6 and 7. These reactions were studied under pseudo-first-order conditions with $Cr^{2+}$ in excess. For *N-meso*-$L^1CoR^{2+}$, the absorbance decrease was monitored at 480 nm; for $L^2CoR^{2+}$, the increase at 390 nm (the maximum for $CrR^{2+}$) was monitored.

$$LCoR^{2+} + Cr^{2+} \rightarrow CrR^{2+} + LCo^{2+} \quad (6)$$

$$CrR^{2+} + H^+ \rightarrow RH + Cr^{3+} \quad (7)$$

In the latter case, the increase (eq 6) was followed by a decrease as acidolysis (eq 7) proceeds, requiring a consecutive reaction analysis. The analysis established a first-order dependence on [$LCoR^{2+}$]. Plots of $k_{obs}$ vs [$Cr^{2+}$] were linear (Figure 3) with an intercept that represents the value of $k_H$ and a slope equal to $k_6$. The values of $k_6$ are summarized in Table VII.

## Discussion

**Preparation of the Organocobalt Complexes.** The preparation of the new organocobalt complexes is based on the photochemistry of the organocobaloximes, as described in previous work.[5]

The methyl complexes of *N-meso*-$L^1Co$ and $L^2Co$ can also be prepared from the reaction of $LCo^{2+}$ with *tert*-butyl hydroperoxide, and the *N-meso*-$L^1CoC_2H_5^{2+}$ from *tert*-amyl hydroperoxide. The scheme of reactions is as follows:

$$RC(CH_3)_2OOH + LCo^{2+} \rightarrow RC(CH_3)_2O^{\bullet} + LCo(OH)^{2+} \quad (8)$$

$$RC(CH_3)_2O^{\bullet} \rightarrow (CH_3)_2CO + R^{\bullet} \quad (9)$$

$$R^{\bullet} + LCo^{2+} \rightarrow LCoR^{2+} \quad (10)$$

The complexes *N-meso*-$L^1CoR^{2+}$ (R = $CH_2OH$ and $CH_3OCH_2$) were prepared by the reaction of *N-meso*-$L^1Co^{2+}$ with $H_2O_2$ in the presence of methanol or dimethyl ether. Aliphatic radicals are formed, possibly by way of $HO^{\bullet}$ (eq 11), although not necessarily so. A possible scheme is as follows:

$$L^1Co^{2+} + H_2O_2 \rightarrow L^1Co(OH)^{2+} + HO^{\bullet} \quad (11)$$

$$CH_3OR + HO^{\bullet} \rightarrow {}^{\bullet}CH_2OR + H_2O \quad R = H, CH_3 \quad (12)$$

$${}^{\bullet}CH_2OR + L^1Co^{2+} \rightarrow L^1CoCH_2OR^{2+} \quad (13)$$

The decomposition product of *N-meso*-$L^1CoCH_2OH^{2+}$ is formaldehyde, as expected. Attempts to prepare a crystalline sample of this complex were not successful. Elroi and Meyerstein[30] observed a reaction between $L^1Co^{2+}$ and $^{\bullet}CH_2OH$, which they studied by pulse radiolysis at pH 1–6. The product spectrum is very similar to that observed for *N-meso*-$L^1CoCH_2OH^{2+}$ in this study. However the pulse-radiolytically produced material decomposes in a first-order process with $k = 0.10$ s$^{-1}$, whereas our complex is stable for hours. The reason for the different behavior is not clear. It is possible that a different isomer of the starting $L^1Co^{2+}$ species was used in the previous work.[30] The ready isomerization of $L^1Co^{2+}$ has been recognized only recently.[38] Alternatively, if the same isomer was involved in the two studies, it is possible that the resulting *N-meso*-$L^1CoCH_2OH^{2+}$ reacted with some component of the pulse-radiolytic solution.

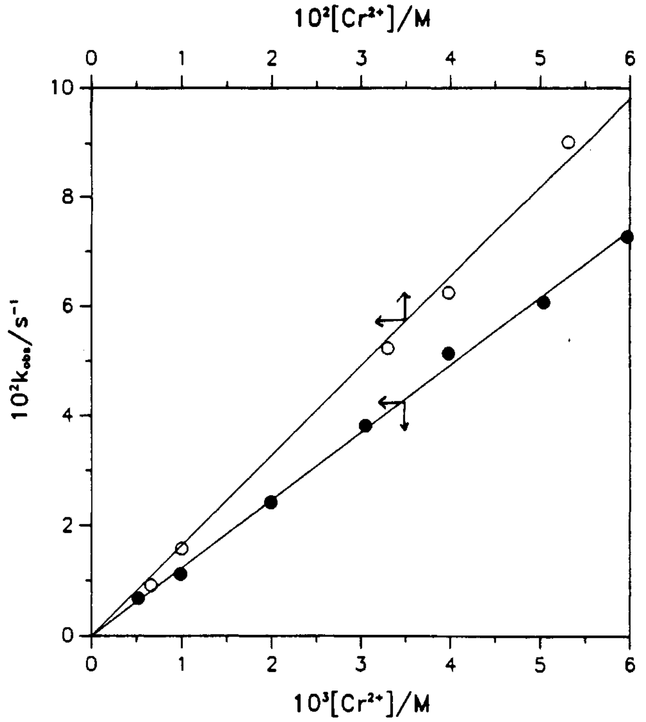

**Figure 3.** Dependence of $k_{obs}$ on [$Cr^{2+}$] for the reaction of $Cr^{2+}$ with $L^1CoCH_3^{2+}$ (filled circles) and $L^2CoCH_3^{2+}$ (open circles).

**Table VII.** Summary of Kinetic Results for the Reaction of $LCoR^{2+}$ with $Cr^{2+}$

| $LCoR^{2+}$ | $k_6$,[a] M$^{-1}$ s$^{-1}$ |
|---|---|
| *N-meso*-$L^1CoCH_3^{2+}$ | $12.3 \pm 0.2$ |
| *N-meso*-$L^1CoC_2H_5^{2+}$ | $(3.6 \pm 0.2) \times 10^{-2}$ |
| *N-meso*-$L^1CoC_3H_7^{2+}$ | $(5 \pm 1) \times 10^{-4}$ |
| $L^2CoCH_3^{2+}$ | $1.64 \pm 0.03$ |
| $L^2CoC_2H_5^{2+}$ | $(5.4 \pm 0.4) \times 10^{-3}$ |

[a] At $T = 25.0 \pm 0.1$ °C and $\mu = 1.0$ M.

A modified Fenton reaction (eqs 11–13) was also used to prepare *N-meso*-$L^1CoCH_3^{2+}$ from dimethyl sulfoxide. Similarly, absorption peaks suggesting an organocobalt complex were observed when *tert*-butyl alcohol was present in the reaction of *N-meso*-$L^1Co^{2+}$ with $H_2O_2$. Attempts to isolate this product, which we presume to be *N-meso*-$L^1CoCH_2C(OH)(CH_3)_2^{2+}$, were not successful, since it decomposes in about 30 min. The possible decomposition reaction is

$$L^1CoCH_2C(OH)(CH_3)_2^{2+} + H^+ \rightarrow (CH_3)_2C{=}CH_2 + L^1Co^{3+} \quad (14)$$

Unfortunately, the same method does not work for other free radicals such as $CH_3\dot{C}HOH$ (from ethanol) or $^{\bullet}CH_2CHO$ (from ethylene glycol). *N-meso*-$L^1Co^{3+}$ was the only product observed in these reactions.

Attempts to prepare $L^1CoR^{2+}$ for R = $(CH_3)_2CH$, $(CH_3)_2CHCH_2$, $(CH_3)_3CCH_2$, and $PhCH_2$ were made. Neither the photolysis method nor the reaction with the appropriate hydroperoxide yielded an observable organocobalt complex. Presumably the reason for this is that such a product, once formed, is highly unstable. Previous results[5,31] show great differences in stability among the corresponding complexes with L = [14]ane$N_4$; the

---

(30) Elroi, H.; Meyerstein, D. *J. Am. Chem. Soc.* **1978**, *100*, 5540.

(31) Bakac, A.; Espenson, J. H. *Inorg. Chem.* **1987**, *26*, 4307.

benzyl homolyzes rapidly ($k_{298} = 0.094\ \mathrm{s^{-1}}$), the isopropyl is unknown, and the ethyl (and other primary alkyls) is stable for many hours at room temperature. Similarly, Halpern and coworkers[32] found that for L = saloph, the *n*-propyl and isopropyl derivatives differ considerably in stability, with $k_H = 4.7 \times 10^{-4}$ and $5.7 \times 10^{-2}\ \mathrm{s^{-1}}$, respectively, at 70 °C.

**Structure of *N*-rac-$(H_2O)L^1CoCH_2Cl^{2+}$.** The complex has the hydrogen atoms of both amino groups and the coordinated chloromethyl on the same side of the macrocycle.

The cobalt atom lies in the plane defined by the four nitrogen atoms. The Co–N bond length varies with the hybridization of the donor atom as expected:[33,34] 1.92 Å for Co–imine, 1.98 Å for Co–amine. The Co–C bond distance of 1.965 ± 0.005 Å is comparable to those of similar alkylcobalt(III) complexes.[35-37] The Co–O ($H_2O$) bond length for the chloromethyl complex is 2.06 ± 0.04 Å, which is a little shorter than that of *N-rac*-$(H_2O)L^1CoCH_3^{2+}$ (2.115 ± 0.004 Å).[35]

The chloromethyl complex has the terminal methyl groups occupying axial positions in the ring on the same side of the $N_4$ plane as the coordinated water molecule. Therefore it has three sets of inequivalent methyl groups (each set has two equivalent methyl groups). This is consistent with its $^1H$ NMR spectrum, which shows three singlets with the same intensity in the range 0.9–2.2 ppm. This is different from what was[38] found recently for another isomer of the methyl derivative, which has the two methyl groups on the ring on the same side of the $N_4$ plane as the cobalt–methyl bond. The reason is the method of preparation. The radical $^\bullet CH_2Cl$ was captured by the meso cobalt(II) complex, in which the cobalt atom is six-coordinate; subsequent isomerization in neutral solution provided the racemic form, whose structure we report here. The methyl complex in ref 38 was prepared by the reaction of $^\bullet CH_3$ with the racemic cobalt(II) macrocycle in which the cobalt is five-coordinate. The methyl simply adds to the vacant position, affording a different isomer.

**Isomerization of $L^1CoR^{2+}$.** The original radical capture employed the N-meso isomer of the Co(II) complex in acidic solution and yielded the N-meso isomers of the organocobalt products. Changes in the $^1H$ NMR spectra show that the meso isomer converts completely to the racemic in neutral solution, as confirmed by the crystal structure of the chloromethyl complex in addition to the NMR data for R = $CH_3$, $C_2H_5$, and *n*-$C_3H_7$. The isomerization reaction does not occur in acidic solutions, suggesting that it probably proceeds by deprotonation and inversion of a secondary nitrogen.

The isomerization of N-meso and N-racemic isomers of the cobalt(II) complex has been shown to be slow at room temperature ($k < 2 \times 10^{-7}\ \mathrm{s^{-1}}$) in organic solvents and in acidic aqueous solution.[38] Isomerization is rapid in alkaline solution, with the N-racemic form being favored at equilibrium. The same is true of the alkylcobalt derivatives we have characterized.

**Homolysis.** The unimolecular homolysis of *N-meso*-$L^1CoC_2H_5^{2+}$ has been studied carefully with a series of different scavengers. The reaction is shown in Scheme II and eq 15. Under

$$C_2H_5^\bullet + S \rightarrow \text{products} \qquad k_3 \tag{15}$$

the conditions studied (large excess of scavengers), the rate law is given by eq 16, which predicts that the value of $k_{obs}$ should be

$$-d[L^1CoC_2H_5^{2+}]/dt = k_H[L^1CoC_2H_5^{2+}] \tag{16}$$

independent of the identity and concentration of the scavenger used. As shown in Table V, this is the case.

**Table VIII.** Rate Constants and Activation Parameters for Unimolecular Homolysis of Alkylcobalt Complexes $LCoR^{n+}$

| $LCoR^{n+}$ | $k_H$(298 K), $\mathrm{s^{-1}}$ | $\Delta H^\ddagger$, kcal $\mathrm{mol^{-1}}$ | $\Delta S^\ddagger$, cal $\mathrm{mol^{-1}\ K^{-1}}$ |
|---|---|---|---|
| *N-meso*-$L^1CoC_2H_5^{2+}$ [a] | $3.9 \times 10^{-4}$ | 25.1 ± 0.9 | 10 ± 3 |
| *N-meso*-$L^1CoC_3H_7^{2+}$ [a] | $3.3 \times 10^{-4}$ | 26.6 ± 0.9 | 14 ± 3 |
| $C_2H_5Co(Me_6[14]aneN_4)^{2+}$ [a] | $6.7 \times 10^{-4}$ | 25.6 ± 0.6 | 12 ± 2 |
| $C_3H_7Co(Me_6[14]aneN_4)^{2+}$ [a] | $4.4 \times 10^{-4}$ | 26.5 ± 0.8 | 15 ± 3 |
| *n*-$C_5H_{11}$Co(cobalamin) [b] | $1.5 \times 10^{-4}$ | 23.4 ± 0.2 | 2.6 ± 0.1 |
| *n*-$C_5H_{11}$Co(cobinamide) [b] | $1.1 \times 10^{-7}$ | 32.1 ± 0.1 | 17.3 ± 0.4 |
| *n*-$C_5H_{11}Co[C_2(DO)(DOH)pn]$ [c] | $1.3 \times 10^{-7}$ [e] | 32.2 ± 2.0 | 18 ± 6 |
| *n*-$C_5H_{11}$Co(saloph)py [d] | $3.9 \times 10^{-4}$ [e] | 20.3 ± 0.6 | −6.2 |
| $C_3H_7$Co(saloph)py [d] | $2.1 \times 10^{-7}$ [e] | 27.1 ± 1.1 | 2.6 |
| 2-$C_3H_7$Co(saloph)py [d] | $1.5 \times 10^{-4}$ [e] | 21.8 ± 1.0 | −2.9 |

[a] This study. [b] Reference 39. [c] In *o*-dichlorobenzene; ref 40. [d] In pyridine; ref 32. [e] Calculated from $\Delta H^\ddagger$ and $\Delta S^\ddagger$.

All the scavengers used are effective because they react with $R^\bullet$. Oxygen, for example, forms $ROO^\bullet$, which can in turn yield $L^1CoOOR^{2+}$. HTMPO reacts by forming an addition product. $Co(NH_3)_5Br^{2+}$ oxidizes $R^\bullet$ to RBr and alkene. $Cr^{2+}$ forms an organochromium complex whose acidolysis yields alkane.

The values of the activation parameters and rate constants for homolysis of macrocyclic alkylcobalt complexes in aqueous solutions, along with four examples in nonaqueous solvents, are summarized in Table VIII.[32,39,40] The entries for the saloph complexes show that secondary organocobalt complexes decompose much more readily than do primary ones, with $k_H$ values differing by almost 3 orders of magnitude at room temperature. The large value of the rate constant for $L^2CoC_2H_5^{2+}$ suggests that the values found in this study are quite unusual among similar alkylcobalt macrocycles.

**Reactions of $R^\bullet$ with $(H_2O)LCoR^{2+}$ Complexes.** The equivalent distribution of $C_2H_6$ and $C_2H_4$ observed in the decomposition of *N-meso*-$L^1CoC_2H_5^{2+}$ in the absence of scavengers strongly suggests a fast reaction follows homolysis:

$$R^\bullet + LCoR^{2+} \rightarrow RH + R_{-H} + LCo^{2+} \tag{17}$$

This reaction was confirmed by experiments in which ethyl radicals were chemically generated (from $Fe^{2+}$ + *tert*-amyl hydroperoxide) in the presence of *N-meso*-$L^1CoC_2H_5^{2+}$. The organic products are ethane, ethylene, and butane in a ratio of 44:36:20. In the absence of the ethylcobalt complex, where the self-reactions of the ethyl radical occur, the same products are formed in a ratio of 16:13:71.[28] The dramatic decrease in the relative yield of butane indicates that a process other than self-reaction is occurring, strongly supporting eq 17.

The kinetics of eq 17 were determined for the case of R = $CH_3$, with the result $k = 4.1 \times 10^7\ \mathrm{M^{-1}\ s^{-1}}$. The product is exclusively ethane. This reaction is an example of homolytic attack at saturated carbon, a relatively rare reaction.[41] In the coupling of a Grignard reagent with an alkyl halide catalyzed by silver, a homolytic displacement and substitution on alkylsilver was proposed.[42] Johnson et al.[43] found that (allyl)$Co(dmgH)_2$py reacts with $^\bullet CCl_3$ to yield 4,4,4-trichlorobut-1-ene. They also found benzylcobaloxime reacts with the same radical in the same fashion.[44] The same cobaloxime reacts with $^\bullet C(CH_3)_2OH$ to give 1-phenyl-2-methyl-2-propanol ($k = 1.2 \times 10^7\ \mathrm{M^{-1}\ s^{-1}}$).[45] A closely

---

(32) Tsou, T. T.; Loots, M.; Halpern, J. *J. Am. Chem. Soc.* **1982**, *104*, 623.

(33) Endicott, J. F.; Durham, B.; Glick, M. D.; Anderson, T. J.; Kuszaj, J. M.; Schmonsees, W. G.; Balakrishnan, K. P. *J. Am. Chem. Soc.* **1981**, *103*, 1431.

(34) Endicott, J. F.; Lilie, J.; Kuszaj, J. M.; Ramaswamy, B. S.; Schmonsees, W. G.; Simic, M. G.; Glick, M. D.; Rillema, D. P. *J. Am. Chem. Soc.* **1977**, *99*, 429.

(35) Heeg, M. J.; Endicott, J. F.; Glick, M. D. *Inorg. Chem.* **1981**, *20*, 1196.

(36) McFadden, D. L.; McPhail, A. T. *J. Chem. Soc., Dalton Trans.* **1974**, 363.

(37) Glick, M. D.; Kuszaj, J. M.; Endicott, J. F. *J. Am. Chem. Soc.* **1973**, *95*, 5097.

(38) Szalda, D. J.; Schwarz, C. L.; Endicott, J. F.; Fujita, E.; Creutz, C. *Inorg. Chem.* **1989**, *28*, 3214.

(39) Schrauzer, G. N.; Grate, J. H. *J. Am. Chem. Soc.* **1981**, *103*, 541.

(40) Finke, R. G.; Smith, B. L.; Mayer, B. J.; Molinero, A. A. *Inorg. Chem.* **1983**, *22*, 3679.

(41) Ingold, K. U.; Roberts, B. P. *Free Radical Substitution Reactions*; Wiley-Interscience: New York, 1970.

(42) Tamura, M.; Kochi, J. *J. Am. Chem. Soc.* **1971**, *93*, 1483.

(43) Gupta, B. D.; Funabiki, T.; Johnson, M. D. *J. Am. Chem. Soc.* **1976**, *98*, 6697.

(44) Funabiki, T.; Gupta, B. D.; Johnson, M. D. *J. Chem. Soc., Chem. Commun.* **1977**, 653.

(45) McHatton, R. C.; Espenson, J. H.; Bakac, A. *J. Am. Chem. Soc.* **1982**, *104*, 3531.

related example[46] is the reaction between the methyl radical and $CH_3Ni(cyclam)^{2+}$ to yield ethane ($k = 4.7 \times 10^7\ M^{-1}\ s^{-1}$) and the reaction of $Co(nta)R^{2+}$ complexes.[9d]

**Reaction of Alkylcobalt Complexes with $Cr^{2+}$.** The kinetic studies (Table VII) clearly show that there is a bimolecular reaction between these species (eq 6). The rate constants are dependent on the size of the coordinated alkyl group; the remarkable decrease of the rate constant from methyl to ethyl to *n*-propyl indicates the severe steric hindrance in the transition state. The mechanism appears to consist of an $S_H2$ displacement at the saturated carbon atom[16] and has been discussed in the literature.

**Acknowledgment.** This work was supported by the U.S. Department of Energy, Chemical Sciences Division, under Contract W-7405-Eng-82. We are grateful to Dr. Lee M. Daniels of the Iowa State Molecular Structure Laboratory for the crystallographic data and refinement.

**Supplementary Material Available:** Tables of atomic coordinates, crystallographic data, least-squares planes, positional parameters, and general displacement parameters for $[(H_2O)L^1CoCH_2Cl](ClO_4)_2$ and a stereoview of *N-rac*-$(H_2O)L^1CoCH_2Cl^{2+}$ (12 pages); a table of calculated and observed structure factors (12 pages). Ordering information is given on any current masthead page.

---

(46) Sauer, A.; Cohen, H.; Meyerstein, D. *Inorg. Chem.* **1988**, *27*, 4578.

---

Contribution from the Inorganic and Structural Chemistry and Radiochemical Diagnostics Groups (INC-4 and INC-11),
Isotope and Nuclear Chemistry Division, and the Photochemistry and Photophysics Group (CLS-4), Chemistry
and Laser Sciences Division, Los Alamos National Laboratory, Los Alamos, New Mexico 87545,
and Department of Chemistry, University of Pittsburgh, Pittsburgh, Pennsylvania 15260

# Spectroscopy and Structure of Quadruply Bonded Complexes under Extreme Pressure ($Re_2X_8^{2-}$, $Mo_2Cl_4(PMe_3)_4$)

David E. Morris,* C. Drew Tait,* R. Brian Dyer,* Jon R. Schoonover, Michael D. Hopkins,*
Alfred P. Sattelberger,* and William H. Woodruff*

*Received October 12, 1988*

Application of pressure (up to 150 kbar, where 1 kbar = 986.9 atm = 0.1 GPa) to solutions of $Re_2X_8^{2-}$ (X = F, Cl, Br) and $Mo_2Cl_4(PMe_3)_4$ results in smooth, continuous changes in experimental observables related to metal–metal bond length and, for the Re complexes, torsional angle (X–Re–Re–X dihedral angle). Resonance Raman studies show that increasing pressure engenders an increase in the frequency of the metal–metal stretching mode for all of the species studied, and this change is empirically correlated with a decrease in metal–metal bond length. Large red shifts in the energy of the $^1(\delta \rightarrow \delta^*)$ transitions with increased pressure for $Re_2Br_8^{2-}$ and $Re_2Cl_8^{2-}$, in contrast to the relative insensitivity of $Re_2F_8^{2-}$ absorption and $Mo_2Cl_4(PMe_3)_4$ fluorescence transitions, imply a tendency for the former complexes to distort torsionally from an eclipsed configuration toward a staggered configuration due to pressure-induced steric repulsion of the chloride and bromide ligands. Integrated absorption intensities further show that, at higher pressures, even $Re_2F_8^{2-}$ undergoes some torsional distortion, whereas the steric repulsion of adjacent phosphines located at a 90° dihedral angle on opposite Mo atoms prevents $Mo_2Cl_4(PMe_3)_4$ from distorting along the torsional coordinate.

## Introduction

The nature and properties of the $\delta$-component of the metal–metal quadruple bond have been the subjects of numerous experimental investigations in the 25 years following the discovery of this class of dinuclear complexes.[1] While most studies along these lines have been directed at those dimers that possess the eclipsed geometry (limiting $D_{4h}$ symmetry), which is the structural signature of the $\sigma^2\pi^4\delta^2$ ground-state electronic configuration, significant insight into the $\delta$-bond has recently been gleaned from comparisons of the structural and electronic properties of these species with those of compounds possessing noneclipsed (limiting $D_{4d}$ symmetry) geometries. Such comparisons are informative because the $\sigma^2\pi^4$ triple-bond core is cylindrically symmetric and remains intact upon rotation about the metal–metal bond; differences among the properties of these two sets of complexes are thus due to variations in $\delta$-overlap. Structural,[2] magnetic,[3] and spectroscopic[3-5] studies of compounds of the $\beta$-$Mo_2X_4[R_2P(CH_2)_nPR_2]_2$ type, where ligand-backbone strain of the bridging diphosphines induces torsional distortion about the metal–metal bond, have been particularly important in this regard and have yielded estimates of the $\delta$-bond contribution to the metal–metal bond length, the energy of the singlet–triplet $\delta\delta^*$ excited-state splitting, and the relative energy contributions of the one- and two-electron terms to the $^1(\delta \rightarrow \delta^*)$ transition energy.

An alternate approach to using binucleating ligands to induce metal–metal torsional distortions, and one that in principle allows for the production of a continuum of rotational geometries for a single complex, involves the application of high external pressure to quadruply bonded dimers. Three investigations along these lines, all of which focus on the $Re_2X_8^{2-}$ class of quadruply bonded dimers, have recently been reported.[6-8] Unfortunately, a concensus on the interpretation of the effect of pressure on the molecular and electronic structures of these ions has failed to emerge. In the first study of this type,[6] Carroll, Shapley, and Drickamer (CSD) reported that the $^1(\delta \rightarrow \delta^*)$ transition of crystals of $[n\text{-}Bu_4N]_2[Re_2I_8]$ in poly(methyl methacrylate) lost intensity and slightly red-shifted with increasing pressure and that a new band, attributed to the $^1(\delta \rightarrow \delta^*)$ transition of a new isomer, appeared and concomitantly increased in intensity ~1100 cm$^{-1}$ to lower energy. This observation, coupled with an analogous one of smaller

---

* To whom correspondence should be addressed: D.E.M., C.D.T., R.B.D., A.P.S., and W.H.W., Los Alamos National Laboratory; M.D.H., University of Pittsburgh.

(1) Cotton, F. A.; Walton, R. A. *Multiple Bonds Between Metal Atoms*; Wiley: New York, 1982 (and references therein).

(2) Campbell, F. L., III; Cotton, F. A.; Powell, G. L. *Inorg. Chem.* **1985**, *24*, 4384.

(3) Hopkins, M. D.; Zietlow, T. C.; Miskowski, V. M.; Gray, H. B. *J. Am. Chem. Soc.* **1985**, *107*, 510.

(4) (a) Campbell, F. L., III; Cotton, F. A.; Powell, G. L. *Inorg. Chem.* **1985**, *24*, 177. (b) Cotton, F. A.; Dunbar, K. R.; Matusz, M. *Inorg. Chem.* **1986**, *25*, 3641. (c) Cotton, F. A.; Dunbar, K. R.; Poli, R. *Inorg. Chem.* **1986**, *25*, 3700.

(5) Hopkins, M. D.; Gray, H. B.; Miskowski, V. M. *Polyhedron* **1987**, *6*, 705.

(6) Carroll, T. L.; Shapley, J. R.; Drickamer, H. G. *J. Am. Chem. Soc.* **1985**, *107*, 5802.

(7) Morris, D. E.; Sattelberger, A. P.; Woodruff, W. H. *J. Am. Chem. Soc.* **1986**, *108*, 8270.

(8) Carroll, T. L.; Shapley, J. R.; Drickamer, H. G. *J. Chem. Phys.* **1986**, *85*, 6787.

0020-1669/90/1329-3447$02.50/0 © 1990 American Chemical Society